JOURNAL OF MATERIALS SCIENCE 37 (2002) 3155–3161

Freeform fabrication by controlled droplet deposition of powder filled melts

C. AINSLEY, N. REIS, B. DERBY
Manchester Materials Science Centre, UMIST and the University of Manchester, Grosvenor St, Manchester M1 7HS, UK
E-mail: brian.derby@umist.ac.uk

A method of directly delivering highly filled hot-melt particulate suspensions using piezoelectric droplet generators is presented. Highly fluid suspensions of alumina in a mixture of long and short chain *n*-alkanes containing up to 40% by volume solids have been prepared. These fluids were subsequently used to deposit ceramic objects using a commercial ink-jet printer. These objects were then successfully sintered to near full density. The deposition mechanism is controlled by the propagation of acoustic waves in a droplet generating chamber. We have observed the change in resonance of this chamber with the introduction of particles into a fluid. A simple model is developed to explain these observations in terms of changes in the speed of sound of the fluid on the addition of solid particles in suspension.

1. Introduction

Ink-jet printing is now a mature technology and has widespread applications in the fields of printing, product marking and microdosing. Initial work combining ink-jet printing and layered manufacturing for the production of ceramic parts was undertaken by Sachs and co-workers, using a process of selectively printing binders onto powder beds [1]. Evans and co-workers extended this concept by pioneering the direct printing of ceramic suspensions using ink-jet printers [2–4]. Initial studies of direct ink-jet printing used commercial ink-jet printers optimised for text printing, and thus the volume of ceramic powder in suspension was relatively low (<10 volume%). This was because the viscosity of the suspensions had to be low to allow printing using the unmodified printers available. Evans' work used ceramic suspensions in aqueous or alcohol-based media. The liquid carrier media is removed by evaporation from the deposit after printing. Solid objects can be fabricated by overprinting, however the combination of low solid volume, and the need to remove the solvent before deposition of subsequent layers, results in a relatively low rate of growth in the direction normal to the printed plane.

Instead of using inks that dry after printing, it is possible to use a dye or pigmented suspension, which solidifies on impact cooling. This technology, "phase-change inks", was developed to eliminate the drying cycle during document printing, or product marking, with its risk of smudging. In this case, the solidified deposit typically has a greater height than that obtained after drying, thus enabling a faster rate of deposit growth. It is possible to purchase hot-melt printers for pattern making and object visualisation for rapid prototyping applications. These commercial machines are ideally suited for droplet-based rapid manufacturing, as they are capable of building solid objects from a number of standard format CAD files.

Ink-jet printing technology can use two different mechanisms for the formation of drops and their positioning. These are "continuous" ink-jet printing and "drop-on-demand" ink-jet printing. In continuous ink-jet printing a stream of fluid is passed through a small orifice. The stream breaks up into droplets by Rayleigh instability. If an electric charge is imparted to the drops, these drops can subsequently be steered by applying an electrostatic field. Drops not required for printing are captured and recirculated. In drop-on-demand ink-jet printing, the drops are only formed when required and position control is achieved by mechanically placing the printer head above the desired location before drop ejection. Both methods of ink-jet printing have been used successfully to build ceramic objects [3, 4]. Continuous ink-jet printing operates at much faster droplet generation rates than drop-on-demand printers, however, the need to use an electrically conducting fluid and the possibility of contamination during the recirculation process are limitations for ceramic applications. Here we have worked exclusively with a drop-on-demand printing system.

In previous work we have demonstrated the feasibility of developing ceramic filled powder suspensions, in a simple paraffin wax medium, that can be used with commercial ink-jet printers [5]. Suspensions containing up to 30% by volume alumina were successfully used to print small objects with a Modelmaker 6 Pro (Solidscape Inc., Merrimack, NH, USA). However, in order to successfully sinter objects without distortion, it is necessary to print ceramic suspensions with much higher volume particle fractions. The limiting factor

for printing is the rheology of the printed fluid. This is best understood in terms of their Reynolds and Weber numbers [5–8], but in simple terms is effectively limited by an upper viscosity of about 40 mPas with the Modelmaker 6 Pro printing platform.

In this study we describe a methodology to achieve printable ceramic suspensions of alumina with suitable rheological properties for printing, and a volume fraction of particles in suspension sufficient for subsequent sintering. Ink viscosity is the key parameter for successful inkjet printing of ceramics because of the very low pressures (<1 MPa) that are used. These are much lower than pressures used in conventional ceramic forming operations such as injection moulding. Thus we must address a fundamental dichotomy, the need to maximise the volume loading of the suspension while minimising the increase in suspension viscosity that occurs as the volume fraction of particles in suspension is increased.

2. Experimental

2.1. Materials used

Three α-alumina powders have been studied, AES 11C, AES 22S (Sumitomo Chemical Co., Osaka, Japan) and RA203LS (Alcan, UK). Their particle size distributions were characterised by a laser diffraction technique (Mastersizer, Malvern Instruments, Malvern, UK) and found to be monomodal. Mean specific surface area was determined by means of BET analysis (Coulter SA3100, Beckman-Coulter, Fullerton, CA, USA). These results are given in Table I. Fig. 1 is a scanning electron micrograph (XL30 FEGSEM, FEI, Eindhoven, The Netherlands) showing the powder morphology to be a low aspect ratio plate in all three cases.

TABLE I Experimentally determined powder size distributions and surface area

Powder	Distribution percentiles (μm)			Surface area (m^2/g)
	d_{10}	d_{50}	D_{90}	
AES11C[a]	0.1	0.3	1.8	8.3
AES22S[a]	0.2	0.8	1.9	5.1
RA203LS[b]	0.9	1.5	2.4	3.0

[a]Sumitomo Chemical Co., Japan.
[b]Alcan Chemicals, UK.

The ceramic powders were suspended in n-alkane vehicles with melting temperatures between 50 and 60°C (Sigma-Aldrich, Dorset, UK). Low molecular weight alkanes (kerosene) (Fisher Chemicals, Loughborough, UK) were also used as admixtures to modify the suspension viscosity. Earlier work has shown that given the low dielectric constant of the organic media used, suspensions can be stabilised by means of relatively short chain polymeric surfactants. Combinations of primary amine 1-Octadecylamine (Sigma Aldrich, Dorset, UK) and Hypermer LP1, a commercial polyester based surfactant (Uniqema, Everberg, Belgium) provide efficient (stearic) stabilisation for these systems [5–8].

2.2. Preparation and characterisation of the suspensions

The wax was initially melted and subsequently mixed with 1 weight% of Hypermer LP1 and 0.5 weight% of 1-Octadecylamine (based on the weight of the dry powder). These ratios had been identified in previous work as optimum concentrations for minimum viscosity using a powder identical to AES11C [5]. The ceramic powders were then added and the resulting mixtures milled using zirconia beads in polypropylene containers, at temperatures exceeding 100°C for a minimum of 8 hours. Before mixing, the powders were dried for 6 hours at 350°C and then stored at 110°C, to minimise contamination of the powder surfaces by water adsorption. After milling, the suspensions were filtered using a stainless steel wire mesh (mesh count 500) at 130°C. After filtering they were degassed in a vacuum oven at a pressure of about 1 kPa (10 mbar) for 10 minutes, and allowed to solidify and cool down to room temperature for storage.

Viscosity measurements were carried out at elevated temperature using a co-axial cylindrical geometry viscometer (DV-III+ Brookfield Engineering Laboratories, Middleboro, MA, U.S.A) equipped with a small sample adapter and a re-circulating oil bath. Those experiments involving kerosene mixtures required the use of a vapour trap to minimise losses. Viscosity measurements were carried out at a temperature of 120°C under several imposed steady shear rates. The shear rate

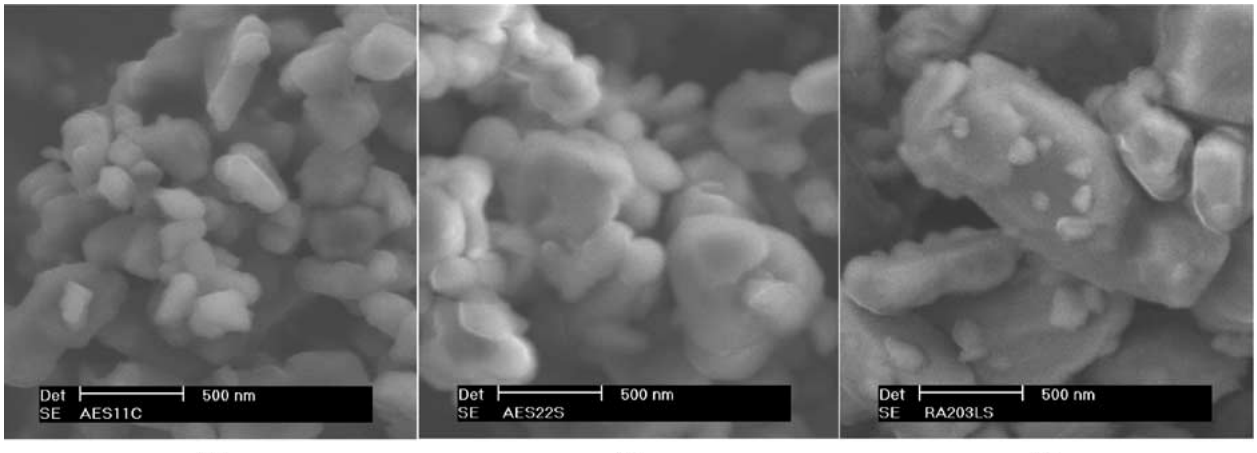

Figure 1 SEM micrographs of the powders used in this investigation.

range was limited by the shear stress developed in the suspension, that range decreasing with increasing particulate content (or increasing viscosity). The melting behaviour of the fluids used to suspend the ceramics was characterised by differential scanning calorimetry (STA 449C, Netzsch Instruments, Selb, Germany).

2.3. Ink-jet printing

All printing was carried out using a Modelmaker 6 Pro (Solidscape Inc., Merrimack, NH, USA), henceforth referred as MM6. This consists of two independent piezoelectric driven ink-jet heads. One head is used to print the ceramic suspension and the second to print a supporting material, "Protosupport" a commercial material supplied by Solidscape Inc. The role of the support material is to provide a base on which the ceramic suspension can be printed. After printing, the support material can be leached away thus allowing overhanging features to be fabricated. Previous work using isolated ink-jet printing heads used in the MM6 had found that the excitation voltage used was insufficient to generate sufficient fluid pressure to eject ceramic suspensions containing 40 vol% particles [5]. Thus, an additional power supply to the original system was introduced in order to increase the voltage pulse used to excite the piezoelectric actuator.

The formation of liquid droplets during ink-jet deposition was characterised by monitoring a single jet using a dedicated Jet Test Station. This consists of a single drop-on-demand piezoelectric jet head assembled with a heating jacket (Sanders Design International, Wilton, NH, USA). This apparatus allows control of the driving pulses used to fire the ink-jet (pulse amplitude, duration and peak shape) as well as the fluid temperature. Drops can be imaged using a stroboscopic system synchronised with the ink-jet firing pulse. The stroboscopically back lit images are captured using a CCD camera system. Mean droplet velocity can be determined from the spacing between the droplets and the frequency of operation. Mean droplet mass can be determined by collecting and weighing a known large number of drops after printing.

3. Results and discussion

3.1. Rheological considerations

In order to achieve a lower viscosity suspension of ceramic particles there are three strategies that can be followed.

1. Suitable surfactants can be identified to stabilise the suspension and these are then optimised to discover a minimum in viscosity. This approach was reported in an earlier paper [5] and will not be pursued further here.

2. The viscosity of the suspending medium ultimately limits the viscosity of a ceramic suspension—at least at concentrations below that at which significant interparticle contact occurs. Thus, in an alkane wax based system it is possible to reduce the viscosity of the liquid by reducing the mean carbon chain length.

3. It is well known that the rheology of particle suspensions can be strongly influenced by the mean particle size in suspension. Generally, for particles of similar morphology, larger particles (max size 5 micron) show lower viscosity at the same suspended fraction than do small particles [9].

The effect of reducing the suspending phase viscosity was evaluated through incremental additions of kerosene to the original paraffin wax media. These substances are chemically identical (composed of aliphatic $-CH_2-$ chains) and differ only in molecular length (kerosene is C_{12} and the wax used is approximately C_{30}). Therefore they are expected to be perfectly miscible and exhibit identical affinities to the surfactants used. Moreover, the melting point of the mixtures did not vary considerably with large additions of kerosene by volume, e.g., pure wax melted at 56°C and kerosene:wax of 30 : 70 melted at 50°C. Because of the very similar chemistry of the kerosene modified waxes to the pure wax (both are simple aliphatic hydrocarbons) we do not expect there to be any difference in the behaviour of the surfactants used and we assume that the optimum composition of the surfactants, identified earlier [5], is still appropriate. Fig. 2a shows a clear reduction in viscosity, as increasing amounts of kerosene are added to the wax. In Fig. 2b we can see that the asymptotic high shear rate viscosity of the suspensions scales with that of the wax. Additions of 30% kerosene to the suspension result in a 40% by volume alumina suspension that is below the viscosity threshold for printing using the MM6 (40 mPas).

The influence of particle size on suspension viscosity was investigated using three different pure alumina powders as detailed in Table I and Fig. 1. These have median particle size of 0.3, 0.8 and 1.5 μm but with similar relative particle size distributions. Fig. 3 shows the influence of average particle size on the suspension viscosity. As expected the larger particle size powder showed the lowest suspension viscosity. The viscosity data for the 1.5 μm median particles is very close to the limiting viscosity for successful printing.

It was decided to proceed with printing trials using the suspensions with kerosene:wax carriers using the finest powder. This was for two reasons. First we expect the finer particle size powder to show easier sintering. Second, experience has shown that with ceramic particles greater than 1 μm diameter, significant wear of the ink-jet printing orifice occurs after continuous printing.

3.2. Suspension jetting characterisation

In the MM6 printer, droplet ejection is achieved by the propagation of acoustic pressure waves generated on rapid volume changes induced by the piezoelectric actuator. In its simplest mode of operation, droplets are ejected by an electric pulse consisting of two subsequent and opposite voltage changes applied across the actuator tube thickness. Upon the first voltage change, the tubular fluid chamber enlarges generating a pressure-decreasing wave travelling towards both ends. The rear of the chamber is open to the fluid supply reservoir and this pulse is reflected as a positive wave propagating back towards the front of the jet. When the second voltage change is applied the chamber shrinks in volume and a positive pressure wave is

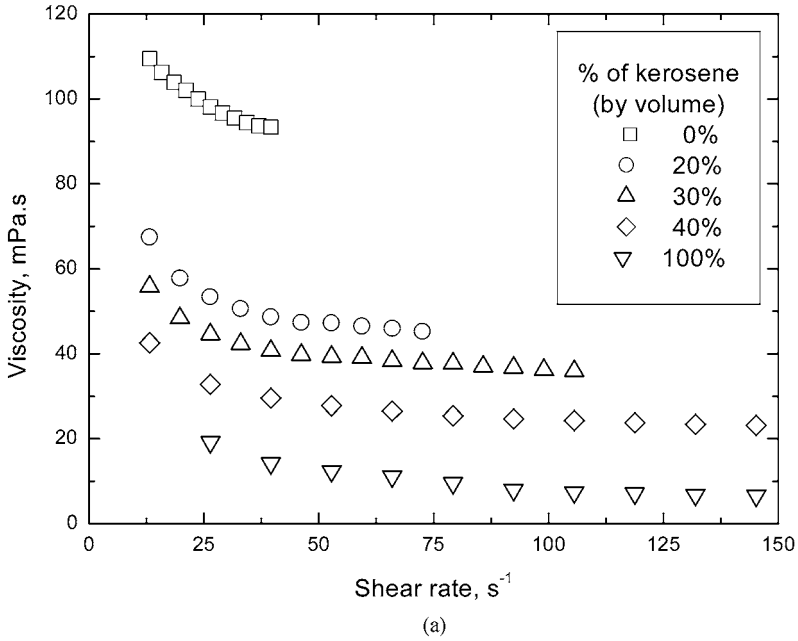

(a)

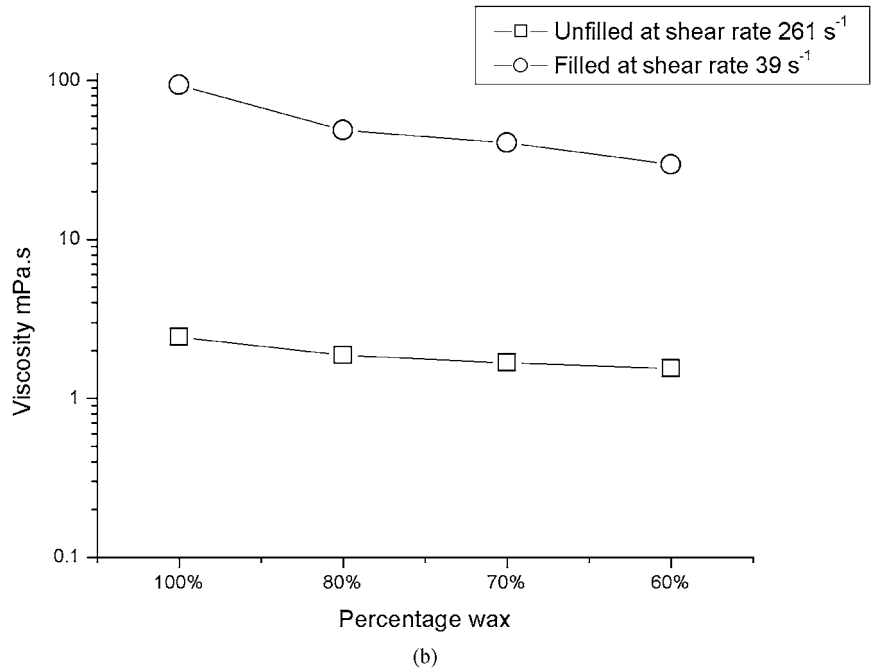

(b)

Figure 2 Viscosity as a function of shear rate for 40 vol% Al_2O_3 suspensions in kerosene:wax carrier vehicles measured at 120°C. (a) Influence of kerosene:wax ratio, (b) comparison of viscosity of suspension with that of the unfilled liquid.

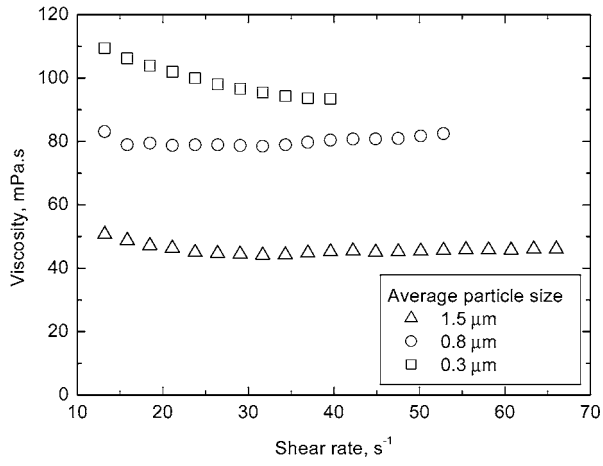

Figure 3 Steady shear viscosity of 40 vol% Al_2O_3 suspension in paraffin wax at 120°C.

generated, again propagating in both directions. When positive waves reach the open printing orifice they displace fluid into a column retained by surface tension forces. If the reflected wave and the second wave interfere constructively this column will be enhanced. Note that the second (compressive) pressure wave travelling to the rear of the jet is reflected as a negative pressure wave and when this reaches the nozzle, the column of liquid is constricted and destabilised. Provided the fluid column had gained enough momentum before the reflected wave arrives at the nozzle, a given amount of fluid detaches from the fluid contained in the chamber, which spheroidises soon after, under the influence of surface tension forces, thus forming a droplet. Clearly an understanding of the response of ceramic suspensions to these pressure waves is necessary to optimise them for use in ink-jet printers.

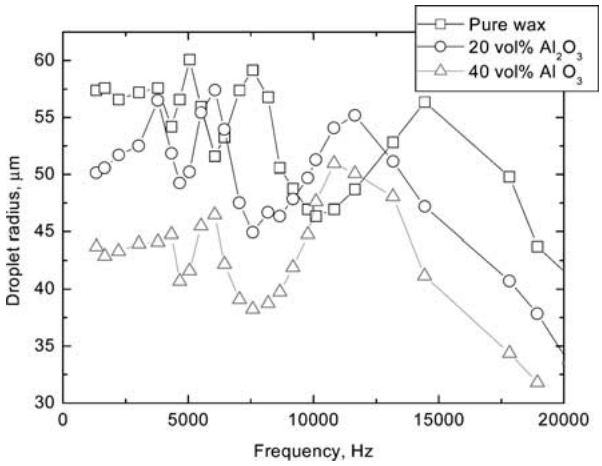

Figure 4 Ejected droplet size as a function of excitation frequency for different levels of filling and keeping all other driving parameters constant (pulse duration and amplitude of 32 s and 60 V, at a temperature of 110°C).

The MM6 was originally designed for operation with simple fluid melts with well-defined properties. In order to print powder filled melts, adjustments must be made to the operating parameters (exciting voltage, peak shape and frequency), to account for their different behaviour. One of the key parameters for ink-jet printing is the frequency response of the filled inks (dynamic resonance behaviour) since this will dictate the optimum electric pulse frequency range used to excite the piezoelectric transducer. Fig. 4 shows the dependence of ejected droplet size on excitation frequency for unfilled, 20 vol% and 40 vol% alumina suspensions. Note that both droplet size and resonance frequency (represented by the peaks in each curve) decrease with increasing volume fraction of solids in suspension. The first observation can be explained by dimensionless analysis of the fluid flow characteristic of ink-jet processes, using the ratio between surface tension to viscous forces, N, (sometimes referred to as the ratio between the Reynolds number and the Weber number) [5]:

$$\mathrm{N} = \frac{\sqrt{\gamma \rho\, d}}{\mu} \tag{1}$$

where d is a characteristic length (taken here as the orifice radius) and ρ, γ and μ are the density, surface tension and viscosity of the fluid, respectively. Under the assumption that surface tension does not change significantly due to the presence of particles, the non-dimensional number N decreases by about one order of magnitude from 10 to 1 as the pure wax is filled with 40% by volume particles [5]. This is largely caused by the increase in viscosity of the fluid with increasing volume fraction in suspension. As this characteristic number becomes smaller, the influence of viscous forces (dissipation) becomes more important, hence larger pressure pulses are required to eject identical amounts of fluid with a given momentum. Thus, under identical driving conditions, using a fluid with a lower value of N, the ejected droplet will have lower momentum, which will be manifest as either a lower velocity or smaller droplet radius (mass).

The change in the resonant frequencies observed in Fig. 4 with increasing particle volume fraction in suspension is interpreted as an effect of the change in acoustic wave speed. An expression for the acoustic wave speed (a) for pressure transients inside deformable pipes is given by [10]:

$$a = \frac{c}{\sqrt{1 + \dfrac{Kd}{Eh}\mathrm{C}_1}} \tag{2}$$

where K is the fluid bulk modulus, d and h are the tube diameter and wall thickness respectively, c is the intrinsic speed of sound in the fluid (defined by $c^2 = K/\rho$ with ρ being the fluid density), E the tube material Young's modulus, and the constant C_1 the appropriate correction factor for a tube axially constrained against longitudinal movement:

$$\mathrm{C}_1 = \frac{2h}{d}(1+\nu) + \frac{d}{d+h}(1-\nu^2) \tag{3}$$

where ν is Poisson's ratio. In this case, with the materials and dimensions of the ink-jet printing head [11], $\mathrm{C}_1 \approx 3$. Here, simple rule of mixtures values have been assumed for the density of the suspension and, in terms of bulk compliance, for the bulk modulus:

$$\rho_{\mathrm{eff}} = \phi\rho_{\mathrm{Solid}} + (1-\phi)\rho_{\mathrm{Liquid}} \tag{4a}$$

$$\frac{1}{K_{\mathrm{eff}}} = \frac{\phi}{K_{\mathrm{Solid}}} + \frac{1-\phi}{K_{\mathrm{Liquid}}} \tag{4b}$$

where ϕ is the powder volume fraction and the subscripts indicate the solid or liquid value of the physical constant.

Using the formalism above, the acoustic wave speed in the jets used for the present experiments was calculated as a function of the solids content. Fig. 5 shows the predicted results after substituting Equations 4a and b into Equation 2 and using the following data: $K_{\mathrm{Solid}} = 250$ GPa, $K_{\mathrm{Liquid}} = 1$ GPa, $\rho_{\mathrm{Solid}} = 4000$ kgm^{-3}, and $\rho_{\mathrm{Liquid}} = 800$ kgm^{-3}). Thus as the solid content of the suspension increases, the

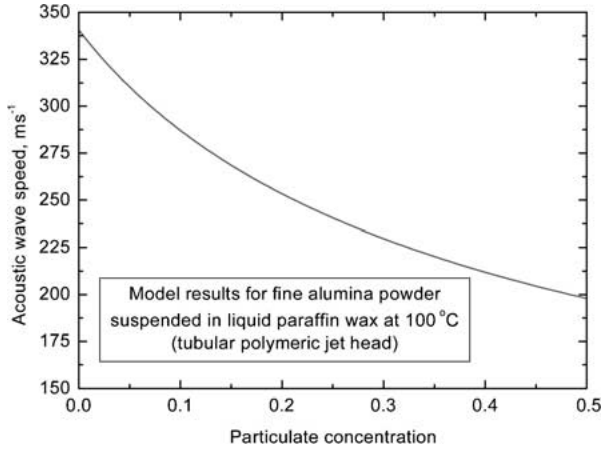

Figure 5 Theoretical prediction of the acoustic wave speed as a function of solids loading.

acoustic wave speed decreases monotonically within the range of interest for printing. The resonances observed in Fig. 4 occur because of acoustic interference within the printing reservoir immediately behind the printing orifice. The dimensions of this reservoir are independent of the fluid used. Therefore for a given frequency of excitation, the wavelength of the acoustic waves becomes smaller as the alumina content of the suspension is increased. Thus the condition of resonance (wavelength matching chamber dimensions) will occur at lower frequencies as the volume content of particulate in suspension increases. This is in agreement with the behaviour observed in Fig. 4.

3.3. Printing of ceramic parts

The information obtained during testing was used to adjust the settings within the ink-jet printer, to account for the different flow and acoustic properties of the filled inks. The MM6 uses vector mode printing, in which case the object is built up a plane at a time with the features in the plane defined by a series of lines—the vectors. In order to produce well defined lines in vector mode, the drops must be placed at an accurately defined separation

Given that the mechanical positioning system cannot operate at constant velocity but must accelerate and decelerate during the printing process, the frequency at which droplets are generated must be altered as a function of horizontal velocity in order to maintain constant drop spacing after impact. Thus it is imperative that the printing conditions, especially drop ejection velocity and drop diameter, be reasonably stable up to the constant velocity frequency (e.g., for a dot pitch of 25.4 μm at a velocity of 101 mm s^{-1}, the maximum frequency at constant velocity is approximately 4 kHz). However, when printing with the 40 vol% suspension, jetting becomes unreliable in the anti-resonance region at about 6–8 kHz (note the valley in Fig. 4). Operation within this range inevitably leads to wetting of the outer face of the orifice and consequent anomalies in the jetting behaviour, effectively limiting the velocity of the print-head traverse. Hence, when re-programming the software driver of the MM6 for use with filled fluids, well determined frequency ranges, and thus traverse velocity ranges, are explicitly prohibited to avoid malfunctions.

Fig. 6 shows a small ceramic impeller of diameter approximately 28 mm obtained by direct printing with 40 vol% alumina suspended in a paraffin/kerosene mixture. This object was printed at a maximum frequency of approximately 5 kHz. It was then given a low temperature heat treatment, in a carbon black powder bed, of 48 hours at 45°C followed by 24 hours at 55°C to remove the wax/kerosene suspending vehicle. This was then followed by a sintering cycle with a maximum temperature of 1600°C held for 1 hour. The final sintered object displayed a linear shrinkage of 18% and a final sintered relative density of 80%.

This rather low sintered density was found to be caused by a large porosity associated with the printing process. The solid object formed by printing consists of a series of beads formed by the coalescence of solidified droplets as the print-head traverses. These beads show uniform parallel sides if the appropriate printing and traversing conditions are chosen [6] and their width depends on the extent to which the droplets spread on impact before solidification. Droplet spreading is a complex function of droplet fluid properties, heat transfer, droplet size and velocity [5]. Thus the width of any printed bead is a complex function of fluid properties and printing conditions. To build a solid object, parallel beads must also coalesce to form a uniform deposited layer. The density of the sintered object is seen to vary with greatest porosity being found close to the top surface (i.e., the layers printed last). This behaviour is believed to show that the beads deposited during later stages of printing show different spreading behaviour and leave larger voids between them. This in turn is thought to indicate different heat transfer conditions, which influence spreading dynamics, as the thickness of the part increases. The part shown in Fig. 6 is approximately 10 mm thick after printing. Smaller objects were found to have greater relative density after printing.

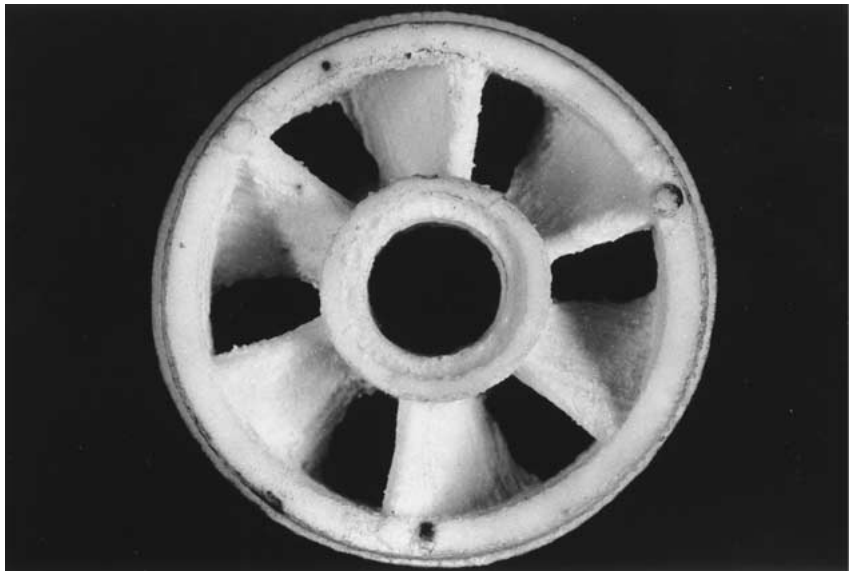

Figure 6 Sintered ceramic impeller, obtained by direct ink-jet printing.

4. Conclusions

We have successfully demonstrated the feasibility of fabricating ceramic objects using ink-jet printing to prepare the desired shape prior to firing. The limiting factor for printing objects is the conflicting requirements of a low fluid density with a large fraction of solids in suspension. By using low melting point mixtures of linear alkanes it is possible to achieve the desired properties with a sub-micron alumina powder available commercially using readily available surfactants. Further work is required to optimise the printing process to minimise the presence of voids that may result because of poor space filling.

Acknowledgements

We acknowledge the financial support of the EPSRC through grant GR/N13784 and the ONR through award N00014-00-1-0737. We thank Sanders Design International, Rolls Royce and Howmet for helpful discussions and support in-kind. Finally we would like to thank Prof. J.R.G. Evans and Prof. J.W. Halloran for many helpful discussions during the course of the project.

References

1. E. SACHS, M. CIMAA, P. WILLIAMA, D. BRANCAZIO and J. CORNIE, *Journal of Engineering for Industry-Transactions of the ASME* **114** (1992) 481.
2. P. F. BLAZDELL and J. R. G. EVANS, *Journal of Materials Processing Technology* **99** (2000) 94.
3. C. E. SLADE and J. R. G. EVANS, *J. Mater. Sci. Lett.* **17** (1998) 1669.
4. Q. F. XIANG, J. R. G. EVANS, M. J. EDIRISINGHE and P. F. BLAZDELL, *Proceedings of the Institution of Mechanical Engineers* B **211** (1997) 211.
5. K. A. M. SEERDEN, N. REIS, J. R. G. EVANS, P. S. GRANT, J. W. HALLORAN and B. DERBY, *J. Amer. Ceram. Soc.* **84** (2001) 2514.
6. N. REIS, K. A. M. SEERDEN, B. DERBY, P. S. GRANT, J. W. HALLORAN and J. R. G. EVANS, in "Solid Freeform and Additive Fabrication," edited by D. Dimos, S. C. Danforth and M. J. Cima, *MRS Symp. Proc.* **542** (1999) 147.
7. N. REIS and B. DERBY, in "Solid Freeform and Additive Fabrication—2000," edited by S. C. Danforth, D. Dimos and F. B. Prinz, *MRS Symp. Proc.* **625** (2000) 117.
8. B. DERBY, N. REIS, K. A. M. SEERDEN, P. S. GRANT and J. R. G. EVANS, in "Solid Freeform and Additive Fabrication—2000," edited by S. C. Danforth, D. Dimos and F. B. Prinz, *MRS Symp. Proc.* **625** (2000) 195.
9. T. A. RING, "Fundamentals of Ceramic Powder processing and Synthesis" (Academic Press, San Diego, USA, 1996).
10. E. B. WYLIE, V. L. STREETER and L. SUO, "Fluid Transients in Systems" (Prentice Hall, Englewood Cliffs, NJ, 1993).
11. Sanders Design International, Merrimack, NH, USA, private communication.

Received 3 June 2001
and accepted 11 February 2002